University of Victoria Tree-Ring Laboratory

Tree-rings show streamflow drought severity is underestimated on Vancouver Island

Report prepared for Cowichan Tribes
Vancouver Island, British Columbia, Canada

Dr. Bethany L. Coulthard
University of Victoria Tree-Ring Laboratory
Department of Geography
April 2016

Introduction

Vancouver Island is considered water-rich because it receives enormous quantities of rain and snow during winter. However, water scarcity and streamflow drought can occur during summer when demand for water is at its highest and stored water is most limited (Stephens et al. 1992). Summer streamflow droughts have become longer, more severe, and more common on the coast in the last few decades as a result of climate warming (Rodenhuis et al. 2007). In 2014 and 2015 many streams experienced droughts that were worse than any on record (B.C. Ministry of Forests, Lands and Natural Resource Operations 2014; B.C. River Forecast Centre 2015).

Drought impacts to human water use, stream ecology, and the survival of local Pacific salmon populations are now recognized by the provincial government as a critical environmental management challenge (B.C. Ministry of Environment 2010), making up a major component of the province's new Water Sustainability Act (B.C. Water Sustainability Act 2014). Usually, hydrometric data measured in rivers are used to understand normal runoff patterns, and to develop drought management and water supply strategies. However, these datasets are very short on Vancouver Island — a few decades long in most cases. As a result, hydrologists and water managers only have a limited snapshot of how serious 'natural' droughts (droughts that were not caused by human land-use or climate change impacts) have been in the past. In many parts of the world, worst-case scenario droughts have not been anticipated because of short hydrometric records (Meko and Woodhouse 2011).

Drought research design

Paleohydrologists develop reconstructions, or long historical records, of streamflow to give a more accurate picture of how severe natural droughts can be in different watersheds (Loaiciga et al. 1993). In a recent study published in the peer-reviewed journal *Journal of Hydrology* (Coulthard et al. 2016; appended to this document) we used tree-ring data to model summer runoff in several rivers across Vancouver Island back to 1658. Although some rivers, like the Cowichan River, were not directly modeled for our study, our results are relevant to any river influenced by winter snowmelt and summer rainfall located on Vancouver Island, including Cowichan River.

We looked specifically at rivers where summer runoff comes in part from snowmelt, and in part from summer rainfall. To build our models, we used two different sets of tree-ring width records; in one set, tree-ring widths in each year correspond with snow depth, and in the other set tree-ring widths in each year correspond with summer dryness. By combining these two types of tree-ring records and comparing them mathematically with instrumental snow and summer rainfall data, we could

model how much runoff is available from snowmelt and from summer rainfall in each summer from 1658-1997 (the age of the trees). The reconstruction that we developed is very statistically reliable and the most robust of its kind in the province.

Research conclusions

We found that worst-case scenario streamflow droughts in many Vancouver Island rivers are very likely underestimated by hydrologists and water managers. Sixteen natural staremflow droughts have occurred across Vancouver Island since 1658 that were more extreme than any observed in the provincial hydrometric records (Figure 1). This means the existing benchmark for the worst drought in this type of river is likely inaccurate. Further, comparing flow-duration curves from instrumental data and reconstructed data shows not only that these severe droughts *do happen* in Vancouver Island rivers, but also that they are *more likely to happen* than is currently thought (Figure 2).

B.C. snowpacks are declining and summers are becoming warmer and drier (B.C. Ministry of Environment 2015). It is very important to recognize that our reconstruction documents only the most severe *natural* droughts that have happened in the past. A drought of the magnitude that we reconstructed, paired with added pressures from climate change, human water use, and human land-use change (deforestation, agriculture, urbanization) could reasonably exceed any drought in the hydrometric record, and probably any drought in the past ~350 years.

Implications for Cowichan River

It is important to understand exactly how our results apply to the Cowichan River, since we did not directly reconstruct Cowichan River streamflow. First, we used tree ring records that capture regional-scale variations in snow depth and summer dryness that similarly impact streams across all of Vancouver Island. This means that the reconstruction model itself is 'regional' in scale, and represents droughts that are synchronous across Vancouver Island. Second, the Cowichan River runoff regime is slightly different from the regimes that we studied; a smaller proportion of summer runoff comes from snow and a greater proportion comes from summer rainfall. In a given year, droughts on Vancouver Island may be caused by lack of snow, by lack of summer precipitation, or both, depending on climate conditions and the type of streamflow regime. Our models account for both snowmelt and summer dryness. For example, of the sixteen most extreme droughts several were caused primarily by low summer rainfall. This means that unprecedented drought can be expected not only in rivers heavily influenced by snowmelt during the drought season, but also in rivers like the Cowichan that rely primarily on summer rainfall during the drought season.

We recommend that more conservative drought mitigation measures are needed to protect against very severe droughts that occur naturally on Vancouver Island, and that are not currently planned for by water managers. These watersheds are relatively small, so that modest in-stream flow reductions can have large ecological consequences. A major natural drought of the scale that we have reconstructed would not only impact human water use, but could be disastrous for local Pacific salmon populations that are already threatened by habitat loss, prior droughts, and overfishing.

Figures

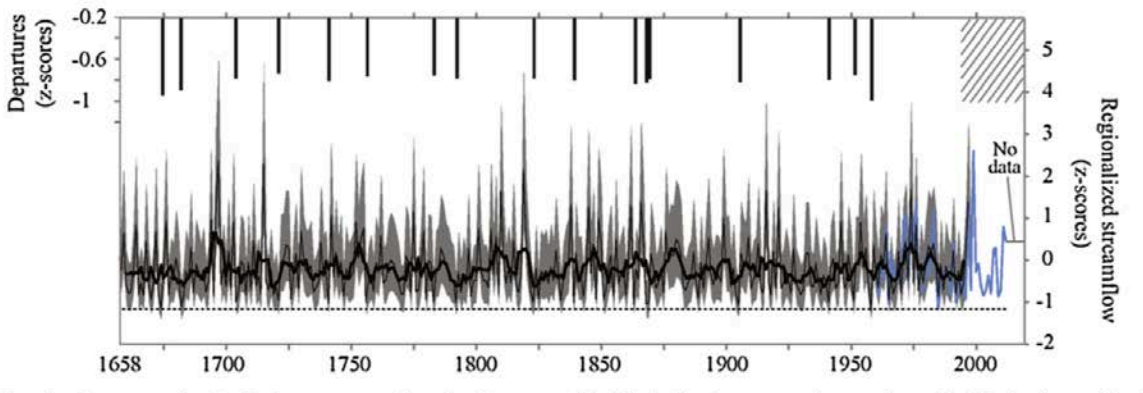

Time plot of regionalized summer streamflow reconstruction, plotted as z-scores (black line) with a five-year running mean (heavy black line), and gauged data (blue line). The grey envelope represents 95% confidence intervals on the reconstruction. The vertical black bars represent sixteen droughts that are more severe than any in the gauged record (calculated as bottom fifth percentile flows relative to the reconstructed instrumental period mean discharge, and plotted as departures from that mean). The bottom fifth percentile flow threshold (z-score<-0.92) is also delineated on the time plot with a black-hatched line.

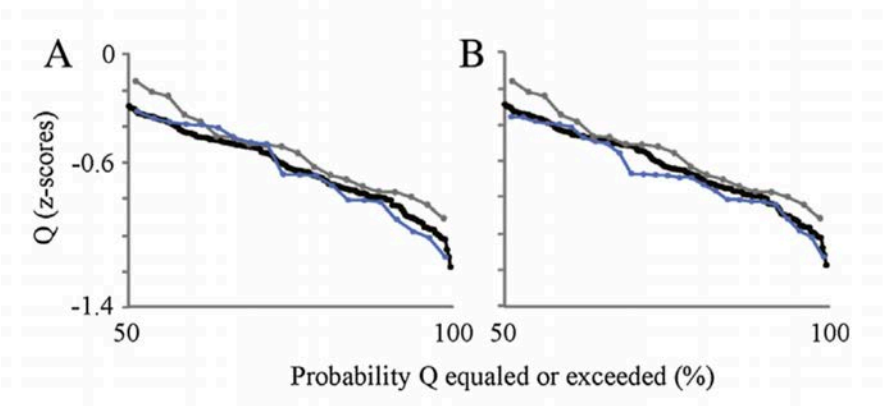

Fig. 7. Flow duration curves of the low flow region only ($p > 0.50$). In panel A the curve from the calibration period hydrometric data (1960–1990; blue line) is compared with curves from the calibration period reconstruction (gray line) and the full-period reconstruction (black line). In panel B hydrometric data from the full available data record (1960–2012; blue line) are compared with the reconstruction curves from panel A.

Works cited

B.C. Ministry of Environment, 2010. Preparing for Climate Change: British Columbia's Adaptation Strategy. From <http://www2.gov.bc.ca/gov/DownloadAsset?assetId=29CDF35B126E483A966B0D5DAE2E3E38&filename=adaptation_strategy.pdf> (retrieved September 25, 2013).

B.C. Ministry of Environment, 2015. Indicators of Climate Change for British Columbia: 2015 Update. From < http://www2.gov.bc.ca/assets/gov/environment/climate-change/policy-legislation-and-responses/adaptation/climatechangeindicators-2015update.pdf> (retrieved April 10, 2016).

B.C. Ministry of Forests, Lands and Natural Resource Operations, 2014. Water Supply and Streamflow Conditions Bulletin. From <http://bcrfc.env.gov.bc.ca/bulletins/watersupply/index-watersupply.htm> (retrieved July 19, 2014).

B.C. River Forecast Centre, 2015. Snow Survey and Water Supply Bulletin. From <http://bcrfc.env.gov.bc.ca/bulletins/watersupply/current.htm> (retrieved June 20, 2015).

B.C. Water Sustainability Act, SBC 2014.

Coulthard, B., Smith, D. J., & Meko, D. M. (2015). Is worst-case scenario streamflow drought underestimated in British Columbia? A multi-century perspective for the south coast, derived from tree-rings. *Journal of Hydrology*. 524, 205-218.

Loaiciga, H., Haston, A., Michaelsen, J., 1993. Dendrohydrology and long-term hydrologic phenomena. Rev. Geophys. 31 (2), 151–171.

Meko, D., Woodhouse, C., 2011. Application of streamflow reconstruction to water resources management. In: Hughes, M.K., Swetnam, T.W., Diaz, H.F. (Eds.), Dendroclimatology. Springer, Netherlands, pp. 231–261.

Rodenhuis D.R., Bennett, K.E., Werner, A.T., Murdock, T.Q., Bronaugh, D., 2007. Climate overview 2007: hydro-climatology and future climate impacts in British Columbia. Report Prepared by the Pacific Climate Impacts Consortium, Victoria, BC. From <http://www.pacificclimate.org/sites/default/files/publications/Rodenhuis.ClimateOverview.Mar2009.pdf> (retrieved September 25, 2013).

Stephens K, Ven der Gulik T, Heath T. 1992. Water, water everywhere: does British Columbia really need a water conservation strategy? The BC Professional Engineer 43(8): 3–7.

Journal of Hydrology 534 (2016) 205–218

Contents lists available at ScienceDirect

Journal of Hydrology

journal homepage: www.elsevier.com/locate/jhydrol

Is worst-case scenario streamflow drought underestimated in British Columbia? A multi-century perspective for the south coast, derived from tree-rings

Bethany Coulthard [a,*], Dan J. Smith [a,1], David M. Meko [b,2]

[a] University of Victoria Tree-Ring Laboratory, Department of Geography, University of Victoria, PO Box 3060 STN CSC, Victoria, British Columbia V8W 3R4, Canada
[b] Laboratory of Tree-Ring Research, University of Arizona, 1215 E. Lowell Street, Tucson, AZ 85721, USA

ARTICLE INFO

Article history:
Received 3 July 2015
Received in revised form 15 December 2015
Accepted 16 December 2015
Available online 21 December 2015
This manuscript was handled by Andras Bardossy, Editor-in-Chief, with the assistance of Bruno Merz, Associate Editor

Keywords:
Drought
Streamflow
British Columbia
Dendrohydrology
Tree rings
Water management

SUMMARY

Recent streamflow droughts in south coastal British Columbia have had major socioeconomic and ecological impacts. Increasing drought severity under projected climate change poses serious water management challenges, particularly in the small coastal watersheds that serve as primary water sources for most communities in the region. A 332-year dendrohydrological record of regionalized mean summer streamflow for four watersheds is analyzed to place recent drought magnitudes in a long-term perspective. We present a novel approach for optimizing tree-ring based reconstructions in small watersheds in temperate environments, combining winter snow depth and summer drought sensitive proxies as model predictors. The reconstruction model, estimated by regression of observed flows on *Tsuga mertensiana* ring-width variables and a tree-ring derived paleorecord of the Palmer Drought Severity Index, explains 64% of the regionalized streamflow variance. The model is particularly accurate at estimating lowest flow events, and provides the strongest annually resolved paleohydrological record in British Columbia. The extended record suggests that since 1658 sixteen natural droughts have occurred that were more extreme than any within the instrumental period. Flow-duration curves show more severe worst-case scenario droughts and a higher probability of those droughts in the long-term reconstruction than in the hydrometric data. Such curves also highlight the value of dendrohydrology for probabilistic drought assessment. Our results suggest current water management strategies based on worst-case scenarios from historical gauge data likely underestimate the potential magnitudes of natural droughts. If the low-flow magnitudes anticipated under climate change co-occur with lowest possible natural flows, streamflow drought severities in small watersheds in south coastal British Columbia could exceed any of those experienced in the past ~350 years.

1. Introduction

In 2014 and 2015 many British Columbia (B.C.) watersheds experienced streamflow droughts that were likely the most severe since streamflow monitoring began in the mid-20th century. Record-breaking low snowpacks and historic high summer temperatures took a particular toll on south coastal basins (Agriculture and Agri-Food Canada, 2014; B.C. River Forecast Centre, 2015). Despite very wet winters, these small watersheds can experience streamflow drought during late summer when snow has melted and weather is warm and dry.

Though they have relatively low storage capacity, small coastal watersheds serve as the primary water source for most communities in south coastal B.C. Many of the streams and rivers in these catchments are also used for hydroelectric power generation, support industry and agriculture, and are critical to the survival of local Pacific Salmon populations. Drought presents a major water management challenge, especially where there is high uncertainty around potential low flow severities (B.C. Ministry of Environment, 2013; Lill, 2002; Mishra and Coulibaly, 2009).

In western Canada, few hydrometric records extend beyond the 1970s. These short instrumental records translate to less accurate estimates of potential low flow severities in a river, and less sound water management strategies (Rodenhuis et al., 2007). Short hydrometric records also make it difficult to determine if recent

* Corresponding author. Tel.: +1 250 580 5551.
E-mail addresses: coulthard.bethany@gmail.com (B. Coulthard), smith@uvic.ca (D.J. Smith), dmeko@ltrr.arizona.edu (D.M. Meko).
[1] Tel.: +1 250 721 7328.
[2] Tel.: +1 520 621 3457.

http://dx.doi.org/10.1016/j.jhydrol.2015.12.030
0022-1694/

droughts are extreme relative to those that occurred in the past. Longer term proxy records of streamflow variability can be estimated from climate-sensitive tree-ring (TR) records by capitalizing upon the influence of climate on both annual radial growth and seasonal runoff (Loaiciga et al., 1993). Dendrohydrological reconstructions can contextualize hydrological changes and inform on connections between modes of regional climatic variability and runoff that are not captured in the instrumental record (e.g., Earle, 1993). The tree-ring based approach is particularly valuable since trees are often distributed over a large hydrological 'sample landscape' and, unlike many other paleoenvironmental proxies (i.e. lake cores, ice cores), information derived from them is annually to sub-annually resolved.

Dendrohydrological modeling has largely been accomplished in dry continental settings, where annual radial tree growth is limited by available soil moisture derived from the same rain and snow meltwater that supports streamflow (Meko and Woodhouse, 2011). The approach is typically applied in large watersheds where errors related to evaporation and 'flashy' rainfall do not contribute to model error (Margolis et al., 2011). Long-term perspectives on hydrological phenomena such as low flows, drought, and long-term runoff declines, have been incorporated into multi-scale and multi-agency watershed management strategies in the southwestern United States (Meko et al., 2001; Woodhouse and Lukas, 2006), western interior Canada (Sauchyn et al., 2014), and internationally (Gou et al., 2010; Norton and Palmer, 1992; Pederson et al., 2001).

Small, temperate watersheds represent a frontier in dendrohydrology due to small basin concentration times, flashy runoff, and an absence of moisture-sensitive tree species (Biondi and Strachan, 2012). In coastal B.C. the approach is hindered further by complex hydroclimatology resulting from mountainous terrain and streamflow contributions from rainfall–runoff, snowmelt–runoff and glacier icemelt runoff. This heterogeneity can lead to differences in seasonal streamflow behavior even in spatially adjacent watersheds (Eaton and Moore, 2010). Previous efforts to establish dendrohydrological records in B.C. have focused on snow- and glacier-melt dominated runoff regimes in continental settings, using moisture-limited TRs (Gedalof et al., 2004; Hart et al., 2010; Starheim et al., 2013; Watson and Luckman, 2005).

In this paper we develop a novel approach for dendrohydrological modeling in small, temperate watersheds in coastal B.C. Despite a lack of moisture-limited trees in this area, the radial growth of some high-elevation conifers is sensitive to annual maximum snow depth as a result of its influence on the length of the growing (energy) season (Peterson and Peterson, 1994). This type of TR data has rarely been used for dendrohydrology. We combine TR width records from a snow depth-sensitive tree species (Mountain hemlock; *Tsuga mertensiana* (Bong.) Carrière; Laroque and Smith, 1999; Gedalof and Smith, 2001; Peterson and Peterson, 2001; Marcinkowski et al., 2015) with a paleoenvironmental record of seasonal drought as predictors in a dendrohydrological model. Our reconstruction targets regionalized summer streamflow in small, hybrid (rain- and snowmelt-driven) watersheds, where summer runoff is driven by a combination of snow meltwater from the previous winter, and summer air temperature and summer precipitation variations. We hypothesized that TR variability and summer discharge in these watersheds are determined by regional-scale climate fluctuations to the extent that TR records can be used as proxies for climate in a model of historical streamflow. We apply the reconstruction to place droughts in long-term perspective, and relate streamflow anomalies to El Niño Southern Oscillation (ENSO; Holton and Dmowska, 1989) events and variations in the Pacific Decadal Oscillation (PDO; Mantua, 2002). Our approach presents an opportunity to develop paleohydrological records for watersheds both smaller in scale and of a different hydrological regime type than those typically conducive to dendrohydrology.

2. Hydroclimatic setting

The regional hydroclimatology of south coastal B.C. is affected by interannual and decadal climate variability driven by ocean–atmosphere interactions in the Pacific Basin, including synoptic-scale modes described by the PDO and ENSO, and to a lesser extent by the Pacific North America (PNA) pattern (Kiffney et al., 2002). Winter storms originating in the North Pacific Ocean deliver moisture to the B.C. coast where it is orographically released upon encountering the Vancouver Island Insular and Coast Mountain ranges, resulting in large quantities of snow and rain. Persistent high-pressure systems typically bring stable warm and dry conditions during the summer months (Stahl et al., 2006).

Atmospheric warming and changing rainfall, snowpack and snowmelt dynamics increasingly moderate these hydroclimate patterns (Barnett et al., 2004; Bonfils et al., 2008). Characteristically mild and wet winters have become milder and wetter over the past 100 years, while summers have become warmer and drier (Pike et al., 2010). Coast and Coast Mountain areas experienced a 1.4 °C rise in mean winter temperature from 1895 to 1995 and winter precipitation (rain and snow) totals are expected to increase by 6% by 2050 (December–February; B.C. Ministry of Water, Land and Air Protection, 2002; Pike et al., 2010). Milder winters and a larger proportion of cool-season precipitation falling as rain have caused widespread snowpack declines; snow water equivalent (SWE) totals diminished by 6% per decade from 1953 to 2000 (B.C. Ministry of Water, Land and Air Protection, 2002; Rodenhuis et al., 2007).

Regional climate trends have altered the seasonal timing and magnitude of peak and low flows, and these changes are expected to intensify in all streamflow regime types (Schnorbus et al., 2014; Stewart et al., 2005). However, hybrid streams are probably most susceptible to earlier, lower, longer, and more frequent low flows over the short term since they are strongly influenced by both warmer and drier summers, and shifting snowpack depth and snowmelt dynamics (Déry et al., 2009; Eaton and Moore, 2010; Loukas et al., 2002; Whitfield and Cannon, 2000). Our use of the term "drought" refers to streamflow drought, a sustained period of below-average stream discharge (Van Loon and Laaha, 2015). Given the low storage capacity of the study catchments, and in keeping with B.C. government environmental management practices, below-average runoff over a period of >1 month is considered streamflow drought (B.C. Ministry of Environment, 2013; Van Lanen et al., 2013).

2.1. Hybrid streams

Hybrid hydrological regimes predominate in south coastal B.C. and are typically found in mid- to low elevation coastal and near-coastal areas. Runoff in these streams is generally highest during winter (November, December, January) as a result of heavy rainfall. A secondary peak occurs in spring (April or May) as a result of snowmelt. Lowest flows occur during summer when inputs from snowmelt are exhausted and regional warm and dry high-pressure systems persist (Eaton and Moore, 2010). Snowmelt can significantly recharge deep flow paths and contribute to summer baseflow, even where a basin contains only a small snow-fed headwater (Beaulieu et al., 2012; Wade et al., 2001). The quantity of discharge in the low-flow season is, therefore, determined by a combination of previous winter snowpack and snowmelt dynamics, summer season precipitation, and summer air temperature.

The proportion of snowmelt- and rainfall-derived runoff in hybrid streams varies year to year, so that the annual runoff pattern may fluctuate from a 'more rainfall-dominated' regime to a 'more snowmelt-dominated' regime (Moore et al., 2007). A high between-year range in flows from month to month is typical (Moore et al., 2007). While winter runoff is flashy in hybrid streams, summer flows are relatively stable due to few rainfall events. This makes them favorable for tree ring-based reconstruction since high-magnitude rains are not typically registered by annual tree growth increments (Meko and Woodhouse, 2011). Summer streamflow in hybrid regimes usually increases during cool/wet La Niñas paired with negative phases of the PDO, while warm/dry El Niño years and positive phases of the PDO usually coincide with a deepening of the Aleutian low, strengthening of the Pacific North America pattern, and reduced winter precipitation and summer runoff (Bonsal and Shabbar, 2008; Fleming et al., 2007; Hamlet and Lettenmaier, 1999). Cool PDO phases exert a strong influence on spring snowmelt dynamics, typically resulting in a later freshet, an increased persistence of meltwater into summer, and generally enhanced summer runoff (Pike and Spittlehouse, 2008).

The climatic drivers of drought in hybrid streams are twofold: (1) less persistence of cool-season moisture into summer as a result of less snowfall, more rain-on-snow events, and earlier spring snowmelt; and, (2) an extension and intensification of the warm dry period between spring and fall rains (Eaton and Moore, 2010). Annual minimum streamflow has decreased in these regimes over the last three decades especially during El Niño years, and low-flow magnitudes are projected to decline by up to 50% by the end of the century (Mantua et al., 2010; Rodenhuis et al., 2007). Profound impacts to stream ecosystem health, Pacific salmon habitat and survivorship (Nelitz et al., 2007; Young and Werring, 2006) and human water use (Barnett et al., 2004; Kay and Blecic, 1996; Kiffney et al., 2002; Mantua et al., 2010; Mote et al., 2003; Nelitz et al., 2007) are documented.

3. Study area

The study area encompasses Vancouver Island and the southwestern slopes of the Pacific Ranges within the B.C. Coast Mountain and islands physiographic region (Valentine et al., 1978). High elevation areas experience short cool summers and long, cool and wet winters typical of a maritime montane climate. Pacific weather systems may deliver greater than 5000 mm of annual precipitation the majority of which falls as snow above 1000 m asl during winter (Pojar et al., 1991). Warm and dry high-pressure systems persist during summer (Valentine et al., 1978).

3.1. Study basins

Following the hydrological classification of Eaton and Moore (2010), we chose four streams susceptible to climate-induced low flows to represent typical small, coastal hybrid flow regimes (Fig. 1). Stream classification was based on analysis of the stream hydrographs (Fig. 2), median and maximum basin elevation, and mean annual discharge values (Table 1). We avoided watersheds characterized by major historical land-use and vegetation change, and those containing natural storage features. Each basin exhibits unprecedented recent (Chemainus River: Craig, 2004; Kanaka Creek Regional Park Management Plan, 2004; Tsable River: Coulthard and Smith, 2015) or predicted (Zeballos River: Déry et al., 2009) summer streamflow drought. Five species of wild Pacific salmon use the rivers for spawning and rearing and have been negatively affected by reduced summer flows (B.C. Conservation Foundation, 2006; Craig, 2004; Gaboury and McCulloch, 2002; Poulin, 2005).

Kanaka Creek is located northeast of the city of Vancouver on the B.C. mainland, where it drains a small area of the Garibaldi Ranges on the northern margin of the Fraser Valley to the Fraser River and Strait of Georgia (Fig. 1; Table 1). The lowermost reaches of the basin are heavily urbanized. The Chemainus River watershed is located on the east coast of Vancouver Island where it drains high-elevation areas surrounding Mts Brenton and Whymper (Fig. 1; Table 1). A band of urban development occupies a small portion of the watershed at the town of Chemainus, where the river flows eastward into the Strait of Georgia. The Tsable River watershed drains the northeastern portion of Beaufort Range on central Vancouver Island, and contains several small lakes including Tsable Lake ($\sim$1 km^2) (Fig. 1; Table 1). Both Chemainus and Tsable rivers experience relatively low mean annual discharge relative to basin size as they are located in the rain shadow of the Vancouver Island Ranges (Moore et al., 2007). Zeballos River is located on the northwest coast of Vancouver Island where it drains the steep western slopes of the Haihte Range to Zeballos Inlet and the Pacific Ocean (Fig. 1; Table 1). The Zeballos watershed contains a small lake and run-of-river hydroelectric project.

Lowest mean monthly discharge in the four watersheds occurs in July and August (Fig. 2). Winter precipitation falls predominantly as rain in the lower portions of the catchments, and as snow above 1000 m asl (Eaton and Moore, 2010). Snow remains in storage until the onset of spring melt, often persisting well into summer at high elevations (Pojar et al., 1991). Industrial logging has occurred throughout all of the watersheds, and remains the dominant human land use in the three Vancouver Island basins.

3.2. Forest stands

The mountain hemlock trees sampled for this study were located between 900 and 1500 m asl within the Mountain Hemlock biogeoclimatic zone (Table 2; Klinka et al., 1991). At this elevation the annual radial growth of mountain hemlock is typically limited by growing season length, which is in turn controlled by snow depth and meltout timing (Gedalof and Smith, 2001; Marcinkowski et al., 2015; Peterson and Peterson, 2001). Seventy percent of annual precipitation falls as snow and deep late-lying snowpacks maintain near-freezing soil temperatures that impede growth often as late as the end of July (Peterson and Peterson, 2001; Pojar et al., 1991). At lower elevations where snow melts earlier mountain hemlock trees may also be sensitive to summer temperature fluctuations, in either the year of or the year prior to growth (Marcinkowski et al., 2015). Climatic growth limitations may be periodically disturbed, for example by fungal pests (e.g. *Heterobasidion annosum*) or hemlock dwarf mistletoe (*Arceuthobium tsugense*) (Means, 1990).

4. Data and methods

A network of mountain hemlock annual TR-width records (chronologies) potentially sensitive to annual maximum snow depth was constructed from TR records developed specifically for this study and additional TR chronologies developed by Coulthard and Smith (2015). These data were combined with an existing grid point-based reconstruction of summer Palmer Drought Severity Index (PDSI; Cook et al., 1999, 2004) to reconstruct summer (July–August) regionalized streamflow for the target basins.

4.1. Tree-ring data

TR data were derived from tree cores collected in fall 2012 and from raw (un-crossdated) digital measurements of previously

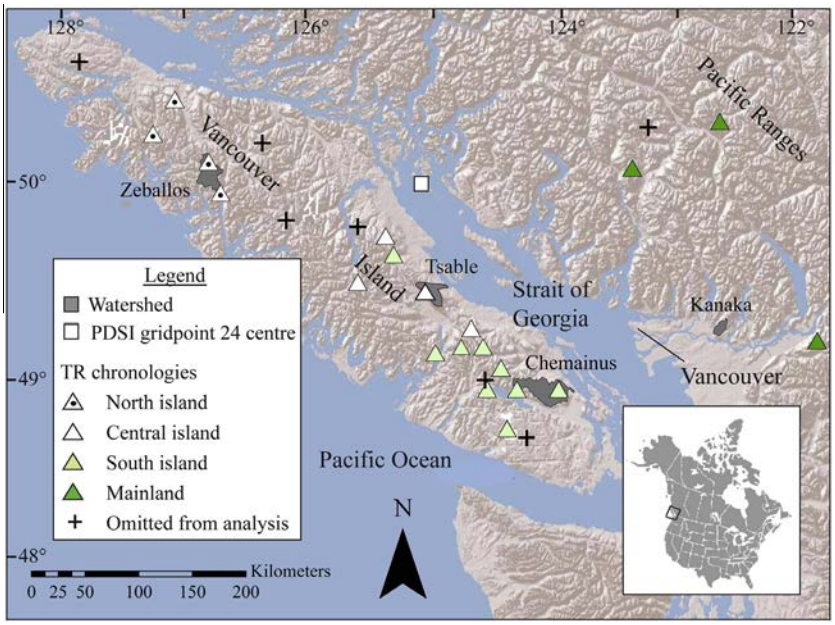

Fig. 1. Map of the study area. Different symbols for TR site chronologies mark members of the four regionalized TR chronologies.

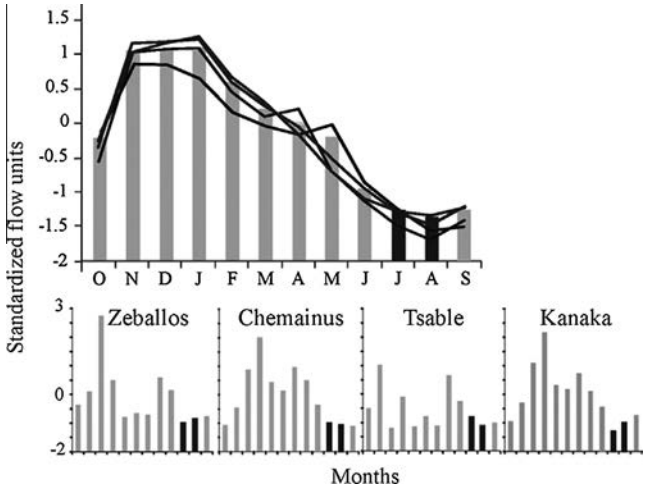

Fig. 2. Above: Annual water-year (October–September) hydrographs of gauged mean monthly discharge over the length of record used (Table 2) for each study basin, in standardized flow units (black lines). Gray bars represent standardized mean monthly discharge averaged across all basins, with the reconstruction season highlighted with black bars. Below: Annual water-year hydrographs of the study streams in years with a strong springtime snowmelt-derived discharge component. The timing of this nival pulse is earlier (April) in the 'more pluvial' Chemainus watershed, a lower-elevation basin where temperatures rise above zero and snowmelt occurs earlier in the season.

collected tree cores archived at the University of Victoria Tree-Ring (UVTRL; Table 2). The TR samples were not necessarily collected at sites within the study watersheds. Rather the primary criterion for site selection was maximization of the sensitivity of annual radial tree growth to regional-scale maximum snow depth variations (Smith and Laroque, 1998; Laroque and Smith, 2003). Two cores were removed from mature trees at standard breast height using a 5.0 mm increment borer, glued to slotted boards, and sanded to enhance annual ring boundaries. Ring widths were measured to an accuracy of 0.001 mm using a Velmex measuring stage system, and crossdated (pattern-matched) using a visual list method that was verified statistically using the program COFECHA 3.0 (Grissino-Mayer, 2001; Holmes, 1983).

TR chronologies were developed using the R package dplR (Bunn, 2008). A long-term age-related growth trend is typically a feature of TR data that must be removed to make inferences about climate-related growth variations (Fritts, 1976). TR width series (measurements from one tree core) were detrended by fitting a cubic smoothing spline with a 50% frequency response at wavelength 100 years to each series and dividing the measured width by the corresponding value of the fitted line (Cook and Peters, 1981). TR growth in the current year is often influenced by conditions in antecedent years (Fritts, 1976). To remove this biological persistence we fit a low-order autoregressive model (Box and Jenkins, 1976) to the TR series, with order identified by the Akaike Information Criterion (AIC). The "residual" TR series (Cook and

Table 1
Study basin information.

River	Station ID	Lat/Long	Gross drainage area (km^2)	Mean annual Q^a (m^3/s)	Median/maximum basin elevation (m asl)
Kanaka	08MH076	49.20 −122.53	48	2.7	230/1050
Chemainus	08HA001	48.87 −123.70	355	18.9	625/1539
Tsable	08HB024	49.517 −124.84	113	7.8	710/1500
Zeballos	08HE006	50.01 −126.84	178	25.9	740/1800

[a] Calculated over the length of record used (1960–1997).

Table 2
Tree-ring chronology information. Regional chronologies in italic font.

Chronology name	Inter-series r[a]	Latitude, longitude	Length (yrs)[b]	Trees, series (#)	Mean r_1[c]
North Island Regional Chronology					
Bulldog Ridge[d]	0.53	50°17′, −127°14′	1845–1997	6, 9	0.72
Castle Mtn.[d]	0.45	50°28′, −127°03′	1845–1997	7, 10	0.75
Colonial Creek[d]	0.43	50°17′, −127°33′	1940–1997	5, 7	0.76
Silver Spoon[d]	0.48	49°58′, −126°40′	1955–1996	8, 11	0.66
N. Isl. Regional[d]	*0.51*		*1630–1997*	*37, 28*	*0.72*
Central Island Regional Chronology					
Mt. Washington[d]	0.63	49°29′, −125°17′	1795–1996	12, 15	0.68
Mt. Apps[d]	0.54	49°26′, −124°57′	1795–1996	22, 40	0.63
Cream Lake[d]	0.61	49°29′, −125°31′	1525–1995	18, 29	0.68
Mt. Arrowsmith[d]	0.63	49°14′, −124°34′	1575–1997	8, 11	0.72
C. Isl. Regional[d]	*0.58*		*1510–1997*	*61, 95*	*0.68*
South Island Regional Chronology					
Mt. Franklyn	0.50	48°54′, −124°11′	1880–1996	16, 28	0.79
Mt. Becher	0.55	49°64′, −125°22′	1668–1997	18, 32	0.76
Mt. Brenton	0.48	48°54′, −123°50′	1726–1996	11, 17	0.77
Pirate Peak	0.54	49°06′, −124°52′	1810–1997	20, 33	0.72
Gemini Mtn.	0.56	49°01′, −124°19′	1850–1996	17, 26	0.64
Mt. Moriarity	0.61	49°08′, −124°28′	1738–1996	20, 36	0.73
Douglas Peak	0.58	49°26′, −124°57′	1750–1996	20, 37	0.82
Wapiti Ridge	0.62	48°54′, −124°26′	1784–1996	21, 38	0.75
TAD Ridge	0.50	48°41′, −124°16′	1720–1996	17, 28	0.75
S. Isl. Regional	*0.54*		*1680–1997*	*160, 275*	*0.74*
Mainland Regional Chronology					
Joffre Lakes	0.61	50°21′, −122°29′	1711–2012	15, 28	0.73
Mt. Cheam	0.70	49°10′, −121°40′	1592–1999	22, 39	0.80
Brandywine	0.67	50°06′, −123°13′	1740–1998	17, 30	0.69
Mainland Reg.	*0.57*		*1658–2012*	*34, 59*	*0.57*

[a] Calculated using the program ARSTAN.
[b] Length truncated where expressed population signal (EPS; Wigley et al., 1984) <0.80.
[c] Mean first-order autocorrelation of all TR series, calculated using the program COFECHA prior to autoregressive modeling.
[d] Developed by Coulthard and Smith (2015).

Holmes, 1986) produced by this procedure have a zero-autocorrelation structure matching that of the streamflow time series we reconstruct in this study. Series from individual cores were combined into single representative regional chronologies using a bi-weight robust mean (Mosteller and Tukey, 1977). Adequacy of the sample size for capturing the hypothetical population growth signal was assessed with the expressed population signal (EPS; Wigley et al., 1984) and chronologies were truncated where EPS fell slightly below the below the standard value of 0.80. The hypothetical growth signal is an estimate of the extent that a TR chronology based on a finite number of trees represents a hypothetically perfect TR chronology based on an infinite number of trees (Wigley et al., 1984).

4.2. PDSI data

The PDSI is a widely used regional drought index that incorporates temperature, precipitation, and soil moisture storage into a single measure of drought severity (Palmer, 1965). Reconstructed annual values of the PDSI for grid cell 24 were downloaded from the NOAA National Climatic Data Center website (2.5° by 2.5° grid cell centered on 50°, −125°; data period used: 1600–1990; http://www.ncdc.noaa.gov/data-access/paleoclimatology-data/datasets; Fig. 1). The 46 drought-sensitive chronologies used by Cook et al. (2004) to generate the moderately strong ($R^2 = 0.37$), well-validated gridpoint-24 PDSI reconstruction are independent from the chronologies used in this study.

4.3. Hydroclimate data

Mean monthly discharge records were downloaded from the Water Survey of Canada website (http://www.wsc.ec.gc.ca/applications/H2O/index-eng.cfm). In addition to fulfilling criteria described previously the study basins were selected based on the length of continuous natural flow data, and a uniform absence of year-to-year statistical persistence during summer months, a statistical feature typical of small coastal basins (Table 3). We seasonalized (summed) the streamflow data (m^3) over July–August for each stream to target the drought season (Eaton and Moore, 2010; Table 3). We calculated z-scores of summer streamflow for each stream over the common data period (1960–2012), created regionally-representative (“regionalized”) data by averaging the records, and applied a log10 transformation where the regionalized data were significantly skewed (Table 3). Regression models were estimated on transformed flows, but are back-transformed and presented as z-scores for plotting and analysis.

We estimated records of precipitation-as-snow (PAS) anomalies on the coordinates of the TR sample sites, and maximum monthly temperature and total monthly precipitation anomalies on the coordinates of the streamflow gauge station sites, using the program ClimateWNA, ver. 4.83 (Wang et al., 2012), which downscales PRISM (Daly et al., 2002) monthly data (2.5 × 2.5 arc min) over the reference period 1961–1990. The PAS data are calculated from average air temperature and total precipitation estimates at a given coordinate location and elevation (Wang et al., 2012). General statistical agreement between the monthly PAS data and snow depth and SWE data from manual snow survey sites, as well as the insufficient lengths of the instrumental snow records for comparison with the tree-ring data, prompted us to use PAS data for the subsequent analysis (stations 3B01, 3B02A, 3B23P, 1D16; http://bcrfc.env.gov.bc.ca/data/survey/). We seasonalized (summed) the PAS data over the period where values were >0 (October through April) as an estimate of annual maximum snow depth, the parameter that most strongly influences tree growth. Climate data were

Table 3
Summer streamflow statistics.

River	Period of record used	cv[a]	skew[b]	r_1[c]	% missing values
Kanaka	1960–2011	0.50	2.15*	−0.17	0.0
Chemainus	1960–2011	0.68	3.78*	0.05	1.9
Tsable	1960–2009	0.70	2.16*	0.07	1
Zeballos	1960–2011	0.33	2.38*	0.03	1.4

[a] Coefficient of variation.
[b] Skewness coefficient; significance at $p < 0.05$ (*) determined by D'Agostino normality test (D'Agostino and Pearson, 1973).
[c] First-order autocorrelation coefficient (none significant ($p < 0.05$) for lags 1–10; Venables and Ripley, 2002).

regionalized by averaging, missing values in both the streamflow and climate data were filled using a long-term mean (<2% of each dataset), and records were truncated where >2 consecutive yearly values were absent.

We used the NOAA Multivariate ENSO Index (MEI) ranks (http://www.esrl.noaa.gov/psd/enso/mei/) and standardized values of the PDO index, downloaded from the NOAA Earth System Research Laboratory website (http://www.esrl.noaa.gov/psd/data/climate indices/list/) to explore the influence of climate modes on streamflow within the instrumental period. We only analyzed values of the PDO index during winter (October through March) months since year-to-year variability in the index is most energetic during that season (Mantua, 2002).

4.4. Diagnostic correlation analysis

As a verification of the assumptions underlying our model, the Pearson correlation coefficient was used to summarize the strength of linear relationships among the TR, streamflow, and climate data. An effective sample size (Dawdy and Matalas, 1964) was used as needed to adjust for persistence in testing correlation for significance.

We first checked whether the individual stream and regionalized summer streamflow data are controlled by the expected climate parameters (annual maximum snow depth, and summer temperature and precipitation). We tested correlations of the streamflow data with previous winter PAS and same-year reconstructed values of the PDSI index, under the assumption that the PDSI operates primarily as a surrogate for summer temperature and precipitation variations. Temporal stability of correlations was tested using a difference-of-correlations test that includes a Fisher's Z transformation of correlations (Snedecor and Cochran, 1989).

Following this we verified that reconstructed PDSI is an appropriate proxy for summer-season temperature and precipitation fluctuations in the study basins. These correlation tests were calculated using the program Seascorr, which summarizes the strength of relationship of annually resolved time series (e.g. PDSI) with monthly and seasonally aggregated climate data and assesses significance of correlation by a Monte Carlo method (Meko et al., 2011). We tested monthly and seasonal correlations between reconstructed PDSI and maximum temperature data for periods ending in each month of the 14-month period beginning in July of the previous year and ending in August of the current year. Partial correlations calculated by Seascorr were then used to identify any influence of seasonal precipitation on the PDSI data independent of the temperature influence.

We also used Seascorr to eliminate from further analysis any of the TR chronologies without significant ($p < 0.05$) linear, temporally stable relationships with previous winter PAS. The TR dataset was reduced further by computing regional TR chronologies from subsets of trees from highly correlated site chronologies. Aggregating chronologies in this way can extend the length of the TR records, and consequently the model prediction period, by enhancing the number of TR series, and the signal-to-noise ratio in the early portion of the data (Cook and Kairiūkštis, 1990). As a final step, Principal Components Analysis (PCA) was run on the regional chronologies to derive independent time series that emphasize common TR variability (Kachigan, 1982). Only the eigenvectors with eigenvalues statistically greater than 1.0 were retained (North et al., 1982). The regional chronologies, PCs of the regional chronologies, and reconstructed PDSI data were evaluated as candidate predictors for the dendrohydrological model.

4.5. Reconstruction model

The reconstruction model was estimated by forward stepwise multiple linear regression of the regionalized July–August streamflow in year t on the pool of predictor variables model in years t, $t + 1$, and $t + 2$. Lags were included to allow TR information in ensuing years to inform on climate conditions in the current year (Cook and Kairiūkštis, 1990). A suite of streamflow models were developed based on various predictor groupings, and evaluated based on explanatory power (adjusted R^2 statistic), model fit and assumptions (analysis of the model residuals, Durbin–Watson and variance inflation factor statistics: DW and VIF), a measure of uncertainty of the predicted values of the model calibration (standard error of the estimate: SE), and an estimate of the statistical significance of the regression equation (F-ratio). Due to the short length of the overall model calibration period we conducted two validation procedures, leave-one-out (LOO) cross-validation and split-period validation. Validation statistics were estimated by comparison of the observed and predicted values for each procedure (Michaelsen, 1987; Snee, 1977). These included the reduction of error (RE; Fritts, 1990), a measure of uncertainty of the predicted values over the validation period (root mean square error of cross-validation; $RMSE_v$), and the Pearson correlation (r) and R^2 of the observed and estimated values. A sign test provided a measure of the number of times the direction of the departures of the annual values from the sample means agreed and disagreed (Cook and Kairiūkštis, 1990). The best model was calibrated on the full period of July–August streamflow data and used to reconstruct regionalized streamflow over the length of the shortest predictor dataset. We used correlation analysis and a previously described difference-of-correlations test to confirm that the predictors selected for our model are linearly correlated with reconstruction-season discharge over the full period of the instrumental record.

4.6. Analysis of the reconstruction

We compared statistical properties of the gauged and reconstructed flows to assess their similarity within and outside the instrumental period. The 0.05 quantile, or fifth percentile, of single-year reconstructed flows was selected as a threshold defining a drought event. To put contemporary low-flows in the context of the instrumental period, we determined the timing and magnitudes of drought events relative to the reconstructed instrumental period mean discharge, and calculated a recurrence interval for these events following the equation of Mays (2005). We compare flow duration curves of the reconstructed and gauged streamflow records to determine if worst-case scenario drought magnitudes and probabilities would be similarly estimated from observed and modeled data. The regionalized flow data and the instrumental period reconstructed record were compared with instrumental records of ENSO and winter PDO over the common data period 1960–1990 to investigate large-scale climatological influences on droughts and wet episodes. A test of proportions (Newcombe, 1998) was applied to determine whether the proportion of years

with below- or above-median runoff during strong El Niño/La Niña years equals the proportion of years with below- or above-median runoff during weak- and non-El Niño/La Niña years. The strength of El Niño/La Niña events was based on MEI ranks (http://www.esrl.noaa.gov/psd/enso/mei/). For winter PDO, the previously described test was used to test for significant difference of correlation (Snedecor and Cochran, 1989) of PDO with streamflow in the cool (1960–1976) versus warm (1976–1990) phases that occurred within our record (Mantua, 2002); effective sample size (Dawdy and Matalas, 1964) was used for this test, as needed, to adjust for autocorrelation in the individual series. A Morlet wavelet analysis on the full period of the reconstructed data highlights localized variations of power over time (Torrence and Compo, 1998).

5. Results

5.1. Tree-ring data

We developed 19 new site-level mountain hemlock chronologies for this study, and also analyzed 10 mountain hemlock chronologies developed by Coulthard and Smith (2015; Table 2). Seven chronologies were omitted from further analysis as they did not meet minimum requirements (chronology information not presented). Interseries correlation values of the detrended series used in the study ranged from $r = 0.43$ to 0.67, indicating strong synchronicity among the records. Analysis of the cross-correlation matrix showed strong statistical agreement among groups of site-level chronologies developed for this study, providing justification for developing two regional mountain hemlock chronologies that represent south Vancouver Island and the south coastal mainland of B.C (Fig. 1). We also used regional chronologies developed by Coulthard and Smith (2015) that represent northern and central Vancouver Island (Fig. 1). The four regional chronologies have series intercorrelation values ranging from 0.50 to 0.57 and minimum (maximum) chronology lengths of 317 (487) years (Table 2). Correlation values among regional chronologies ranged from $r = 0.57$ to 0.74 ($p < 0.01$).

5.2. Diagnostic correlation analysis

Both the individual stream and regionalized summer streamflow records exhibit temporally stable significant positive linear correlations with previous winter PAS and reconstructed values of the PDSI (Table 4). None of the datasets, including PDSI, exhibited significant autocorrelation at lags <10 years. Results of the Seascorr analyses indicate that the reconstructed PDSI record is primarily sensitive to variability in summer temperature and precipitation, and is also weakly associated with precipitation in the previous autumn (Fig. 3A and B). The index exhibits strongest time-stable monthly and seasonal negative correlations with maximum temperature during June–July. A positive correlation with precipitation during June–August is evident (Fig. 3B) from partial correlations that adjust for the strong negative inter-correlation between precipitation and temperature during warm-season months (Fig. 3C). The partial correlations also indicate a strong seasonal pattern in the inter-correlation of monthly precipitation and temperature in the study area, with positive correlation in winter and negative correlation in other months (Fig. 3C). Taken together, these hydroclimate relationships support the interpretation that the study watersheds and the regionalized data derived from them represent hybrid annual flow regimes.

5.3. Reconstruction model

Stepwise regression identified reconstructed PDSI and the first principal component (PC1) of the regional TR chronologies as the best predictors of regionalized summer streamflow. PC1, with same-sign weights (0.92–0.73) on the four regional chronologies, explained 73% of the regional-chronology variance. The final reconstruction model is shown in Eq. (1):

$$Q = 0.235 - (0.100 * \mathrm{PC1}) + (0.041 * \mathrm{PDSI}) \quad (1)$$

The model explains 64% of the variance (adjusted $R^2 = 0.64$) of regionalized summer streamflow, Q, in the 31-year (1960–1990) calibration period. Each model predictor is significantly ($p < 0.01$) linearly correlated with the regionalized streamflow data over the full period of the common record, without the influence of statistical outliers (Fig. 4). The reconstruction spans the period 1658–1990. Values of the standardized regression coefficients indicate that PC1 (−0.602) has a larger effect in determining the dependent regionalized flow values than reconstructed PDSI (0.370). We checked that PC1 was significantly linearly correlated with winter PAS ($r = -0.66$, $p < 0.01$) and that this relationship was stable over time ($p = 0.62$ for the previously described difference-of-correlations test).

Reconstruction, cross-validation, and split-period validation statistics are summarized in Table 5 and the reconstruction is plotted in Fig. 5. Collinearity diagnostics indicate that the model predictors are adequately independent (Table 5), the F-ratio suggests that the regression equation is statistically significant, and positive RE values close to the calibration R^2 values, similar SE and RMSE_v values, and strong relationships between the observed and predicted values of the validation periods indicate a well-validated model (Table 5; Fig. 5). The results of the sign tests indicate the direction of observed and expected departures from the sample means agree significantly more often than would be expected by chance (Table 5).

Analysis of regression residuals revealed no violation of regression assumptions, and suggested generally symmetric error in the estimation of high and low instrumental flows. Visual inspection of the calibration period time plot confirms this, showing over- and under-predictions throughout the record for both high- and low-flow years (Fig. 5). The model is unusually effective for estimating the magnitudes of extreme events, with little compression of the reconstruction variance relative to the instrumental data despite an expectation of compressed variance in TR based regression analysis (Fig. 5; Meko and Graybill, 1995). The magnitudes of lowest instrumental flow years are particularly accurately estimated; no major discrepancies between gauged and reconstructed records occur during those years.

5.4. Analysis of the reconstruction

The basic statistical properties of the regionalized flow data are preserved in the reconstructed instrumental and pre-instrumental records (common instrumental data interval only); autocorrelation

Table 4
Hydroclimate correlations and their temporal stability. Analysis period 1960–1990.

Streamflow data (July–August)	Winter PAS[a]	p[b]	PDSI[c]	p[b]
Regionalized	0.54	0.31	0.59	0.93
Kanaka	0.34	0.74	0.61	0.85
Chemainus	0.59	0.87	0.65	0.37
Tsable	0.60	0.40	0.42	0.97
Zeballos	0.49	0.06	0.36	0.70

[a] Correlation of regionalized streamflow with winter precipitation-as-snow; all correlations significant at 0.01 level.
[b] p-value for a test of the null hypothesis that the population sample correlations in preceding column for the first and second halves of the 1960–1990 period are the same (those split-sample correlations not listed).
[c] Correlation of regionalized summer streamflow with summer reconstructed PDSI at gridpoint 24; all correlations significant at 0.01 level.

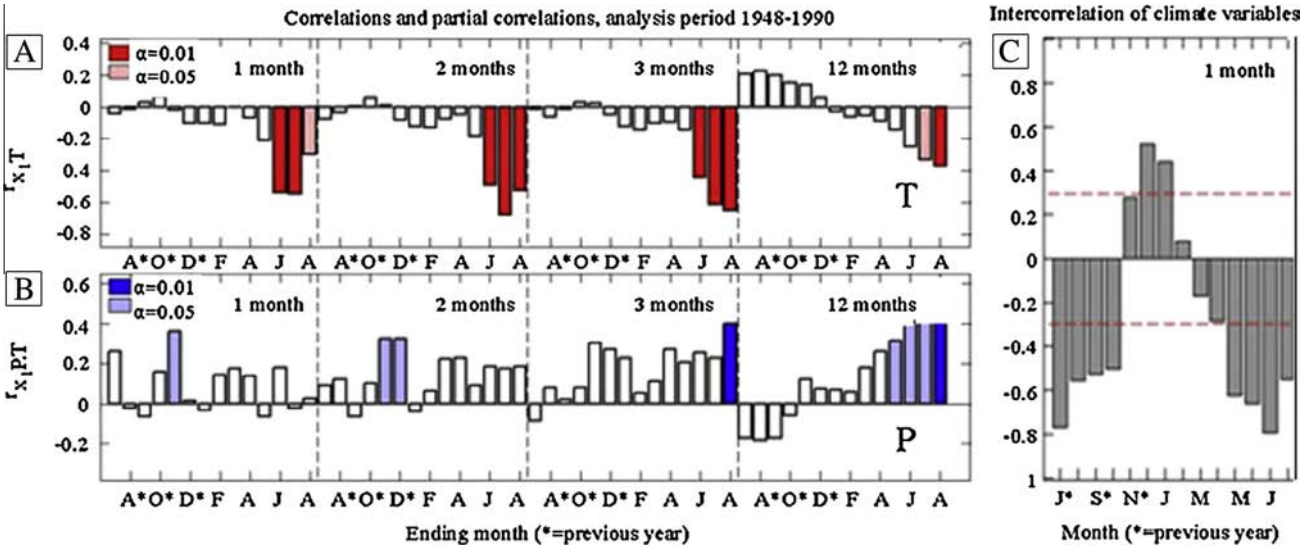

Fig. 3. (A) Monthly and seasonal correlations between reconstructed PDSI and regional maximum temperature (*T*) data, over 1-, 2-, 3-, and 12-month sliding windows beginning in the previous July through current August. The strongest correlation is during June–July ($r = -0.68$, $p < 0.01$). (B) Monthly and seasonal partial correlations between reconstructed PDSI and regional total precipitation (*P*) data, controlling for the influence of T. The strongest independent correlation of reconstructed PDSI with *P* is during June–July–August ($r = 0.65$, $p < 0.01$). (C) Monthly intercorrelations of *T* and *P*. Red-hatched lines represent 95% confidence intervals. All correlations were calculated using Seascorr. (For interpretation of the references to color in this figure legend, the reader is referred to the web version of this article.)

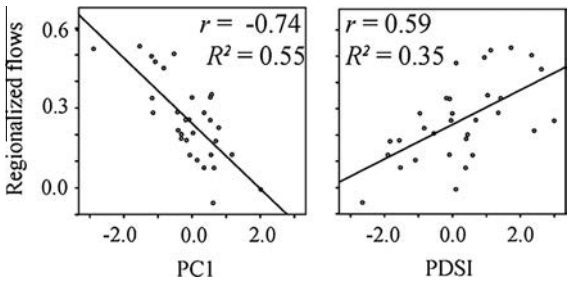

Fig. 4. Scatterplots of the regionalized flow data and PC1 (left) and reconstructed PDSI (right). Correlations significant at the 99% level.

is absent at lags <10 years and mean, minimum, and maximum flows are similar (Table 6). The greatest discrepancy is larger maximum flows in the pre-instrumental period. The instrumental period reconstruction exhibits a similar range of variance to that of the gauged data, while the coefficient of variation (CV) for the instrumental portion of reconstruction is smaller (Table 6). A 5-year running mean highlights generally regularized interdecadal variability in the full-period reconstruction (Fig. 6).

Seventeen bottom fifth percentile flows occurred within the reconstructed record. Remarkably, none of these events occurred during the instrumental period. The reconstruction suggests droughts of this magnitude have a 21-year recurrence interval. The timing and magnitudes of bottom fifth percentile flow years are plotted in Fig. 6 and listed in Table 7, and the flow threshold (z-score < −0.93) is delineated with a black-hatched line on the reconstruction time plot (Fig. 6). Note that for context the hatched line extends beyond the interval of reconstruction into the contemporary period, although these data were not included in the percentile or recurrence interval calculations. Our reconstruction indicates that bottom fifth percentile flows occurred in two consecutive years in 1868 and 1869, and that they did not persist for more than two years at any time. The most extreme single-year departures occurred in 1674, 1682, and 1958, and the magnitudes of these departures exceed any within the gauged record, with the exception of 1985. Flow duration curves (low flow region only, $p > 0.50$) are plotted in Fig. 7. Whether compared with the shorter gauged streamflow record from the calibration period (1960–1990) or the full gauged streamflow record 1960–2012), the reconstruction curve (1658–1990) suggests a higher probability of more severe droughts than the gauge data suggests.

Table 5
Reconstruction, cross-validation, split-period validation, and sign-test statistics.

Reconstruction	R^2	Adj. R^2	D-W[a]	VIF	SE	F-ratio[**]
	0.66	0.64	1.70	1.16	0.09	27.86
LOO validation	RE	$RMSE_v$[b]	r[c]	R^2_v[d]	Sign test (agree/disagree)	
	0.60	0.096	0.78	0.60	27/31[**]	
Split-period validation	RE	$RMSE_v$[b]	R^2_c		Sign test (agree/disagree)	
1960–1974	0.77	0.101	0.76		14/15[**]	
1975–1990	0.55	0.106	0.53		11/16[*]	

[a] Durbin–Watson statistic.
[b] Derived from transformed z-scores of Q.
[c] Cross-validation r ($p < 0.01$).
[d] Cross-validation R^2.
[*] $p < 0.05$.
[**] $p < 0.01$.

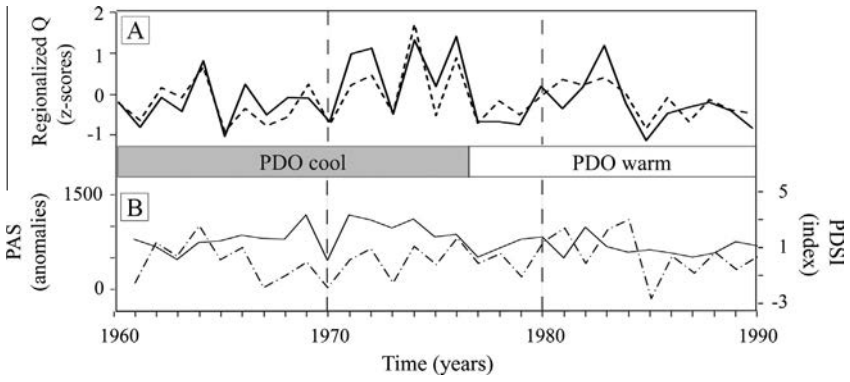

Fig. 5. (A) Time plot of the gauged (black line) and estimated (hatched line) records from the model calibration, and (B) time plot of previous December through March PAS (black line) and reconstructed PDSI (hatched line).

Table 6
Descriptive statistics of gauged and reconstructed flow data, as *z*-scores.

Flow data type (back-transformed)	cv[a]	Mean	Max	Min	r_1[b]
Regionalized gauged	6.4	−0.11	1.41	−1.12	−0.045
Instrumental period reconstructed	5.3	−0.11	1.72	−0.91	−0.160
Pre-instrumental period reconstructed	3.4	−0.19	2.37	−1.18	−0.110

[a] Coefficient of variation.
[b] First-order autocorrelation coefficient (none significant ($p < 0.05$) for lags 1–10; Venables and Ripley, 2002).

Neither the regionalized or reconstructed flows exhibited a significantly different proportion of below- or above-median flows during strong El Niño/La Niña years relative to weak and non-El Niño/La Niña years (Table 8). Both regionalized and reconstructed instrumental period flows were significantly negatively correlated with values of the PDO index during winter (Table 9). Analysis of subperiods revealed that, for both records, the influence of the PDO is stronger during the cool phase of the oscillation, although a test of the difference in correlations between subperiods was only significant for the gauged data. The wavelet power spectrum of the reconstructed flow data identifies significant but intermittent power in the approximately 4- to 10-year bandwidths, energy at approximately 16-year periods in the early part of the record, and an absence of multidecadal variability except in the early 1800s (Fig. 8).

6. Discussion

6.1. Predictor selection and model estimation

Our model effectively estimates variability in regionally-synchronous low-flow season stream discharge for the hybrid watersheds examined in this study. Correlation analyses indicate that: (1) the flow data are driven by variations in previous winter PAS, and summer air temperature and total summer precipitation; and, (2) the selected model predictors serve as proxies for those climate variables.

TR width variability as captured by PC1 operates as a proxy for winter PAS; increased PAS results in a shorter growing season and smaller ring widths, and also promotes greater summer-season runoff. Marcinkowski et al., (2015) found that prior to 2000, energy limitation by late-lying snow was the only time-stable control on the annual growth of mountain hemlock trees in the nearby Cascade Mountains, which is encouraging for the use of this species as a proxy for snowmelt-dominated streams. The authors also report that some post-2000 mountain hemlock trees exhibit a weakened relationship to winter precipitation, possibly due to the increasingly growth-limiting role of climbing spring temperatures, however our reconstruction omits data from that period.

Reconstructed PDSI for gridpoint 24 is sensitive to regional-scale fluctuations in maximum temperature and total precipitation during summer (Fig. 3). In years where values of the PDSI are lower, summer conditions are warmer, evaporation is greater,

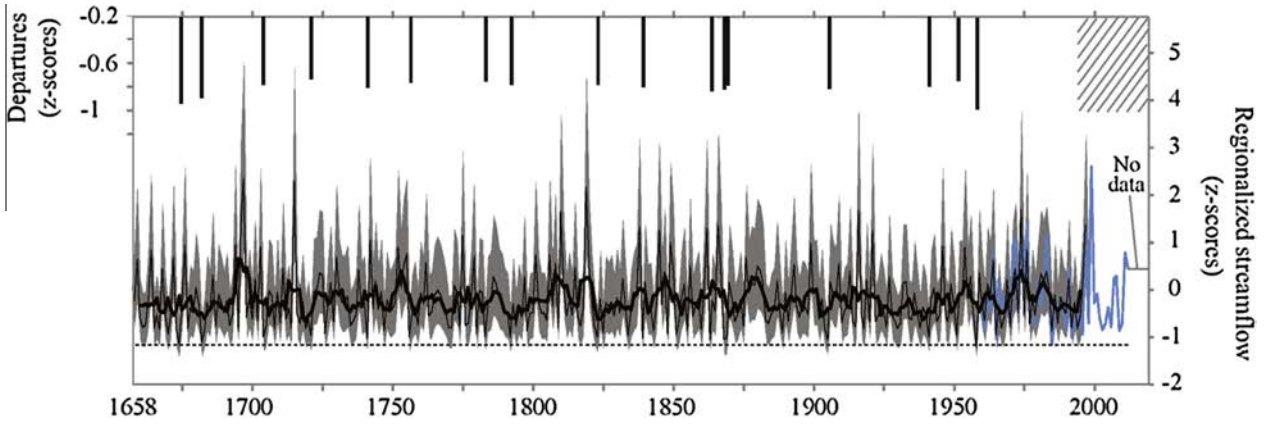

Fig. 6. Time plot of reconstructed regionalized summer streamflow plotted as *z*-scores (black line) with a five-year running mean (heavy black line), and gauged data (blue line). The gray envelope represents 95% confidence intervals calculated from the $RMSE_v$ following the equation of Weisberg (1985). The vertical black bars represent bottom fifth percentile flows relative to the reconstructed instrumental period mean discharge. The bottom fifth percentile flow threshold (*z*-score < −0.92) is delineated on the time plot with a black-hatched line. (For interpretation of the references to color in this figure legend, the reader is referred to the web version of this article.)

Table 7
Lowest reconstructed and gauged flows, listed in order of severity. (A) Pre-instrumental period bottom fifth percentile low flows; (B) lowest gauged flows, with departures calculated from the 1960 to 1990 gauged mean.

	Year	Departure from mean *z*-score	Score
(A)	1958	−0.99	−1.17
	1674	−0.93	−1.11
	1682	−0.89	−1.08
	1905	−0.84	−1.02
	1863	−0.83	−1.02
	1868	−0.83	−1.01
	1839	−0.82	−1.00
	1741	−0.81	−0.99
	1869	−0.80	−0.99
	1792	−0.78	−0.97
	1941	−0.78	−0.97
	1704	−0.78	−0.97
	1756	−0.78	−0.96
	1783	−0.77	−0.96
	1823	−0.77	−0.95
	1951	−0.75	−0.93
	1721	−0.74	−0.93
(B)	1985	−1.01	−1.12
	1965	−0.90	−1.01
	1992	−0.87	−0.98
	1996	−0.80	−0.91
	2009	−0.73	−0.84
	2003	−0.71	−0.82

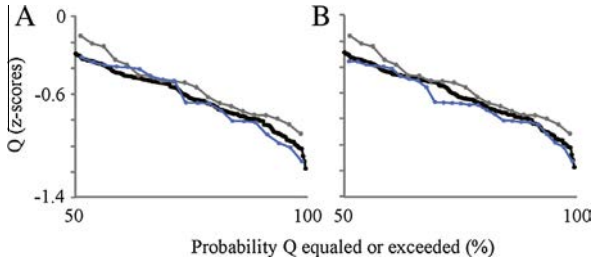

Fig. 7. Flow duration curves of the low flow region only ($p > 0.50$). In panel A the curve from the calibration period hydrometric data (1960–1990; blue line) is compared with curves from the calibration period reconstruction (gray line) and the full-period reconstruction (black line). In panel B hydrometric data from the full available data record (1960–2012; blue line) are compared with the reconstruction curves from panel A. (For interpretation of the references to color in this figure legend, the reader is referred to the web version of this article.)

Table 8
Test of proportions assessing the association of regionalized summer runoff (Q) with El Niño and La Niña events over the period 1960–1990. Calculated using *R* function *prop.test*. Proportions of years in each streamflow category in parentheses. The null hypothesis that groups have the same true proportions was true for all tests, *p*-values ranged from 0.31 to 0.73.

Streamflow category	# El Niño years	# weak/non-El Niño years
Regionalized Q (gauged)		
Below median	5 (38.5%)	14 (56.0%)
Above median	8 (61.5%)	11 (44.0%)
Total	13 (100%)	25 (100%)
Reconstructed Q		
Below median	6 (46.2%)	13 (52.0%)
Above median	7 (53.8%)	12 (48.0%)
Total	13 (100%)	25 (100%)
Streamflow category	# La Niña years	# weak/non-La Niña years
Regionalized Q (gauged)		
Below median	5 (41.7%)	17 (65.4%)
Above median	7 (58.3%)	9 (34.6%)
Total	12 (100%)	26 (100%)
Reconstructed Q		
Below median	7 (58.3%)	12 (46.2%)
Above median	5 (41.7%)	14 (53.8%)
Total	12 (100%)	26 (100%)

Table 9
Associations of regionalized and reconstructed flows with PDO variability over the instrumental period.

	Full period	Cool phase	Warm phase	N_1, N_2[a]	p[b]
Regionalized streamflow	$r = -0.37$ ($p < 0.05$)	−0.67 ($p < 0.05$)	0.08 ($p < 0.05$)	17, 21	0.012
Reconstructed streamflow	−0.35 ($p < 0.05$)	−0.60 ($p < 0.05$)	−0.14 ($p < 0.05$)	17, 21	0.124

[a] Effective sample sizes for early and late periods.
[b] *p*-value for a test of the null hypothesis that the population sample correlations for the cool and warm phases are the same. Significant where $p < 0.05$.

and precipitation and streamflow are reduced. The results of the correlation analyses are consistent with the assumption that the reconstructed annual values of the PDSI serve as a proxy for summer air temperature and to a lesser extent summer precipitation in our reconstruction. Although warmer conditions could

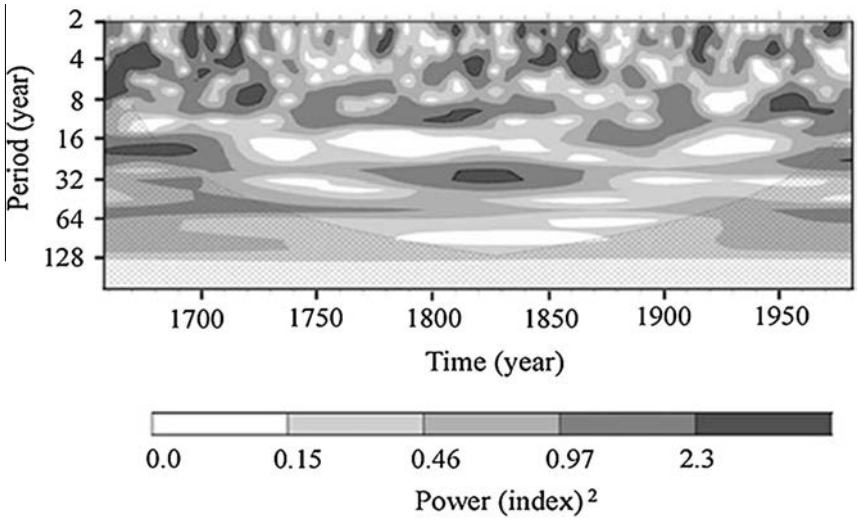

Fig. 8. Morlet wavelet power spectrum on the full-period reconstructed streamflow record. Black contours represent a 95% confidence level based on a white-noise background spectrum. The hatched area represents areas of the spectrum susceptible to the effects of zero padding (Torrence and Compo, 1998).

theoretically increase flow inputs from snowmelt, most snow meltwater is likely in the groundwater system by July–August (Beaulieu et al., 2012).

Because year-to-year streamflow in the small study watersheds is not autocorrelated, we were able to estimate a paleohydrological model based on predictors that inform only on single-year flows, without risking underestimation of an autocorrelated discharge component. In contrast, dendrohydrological models in large basins with slow concentration times can rely on complicated regression models including time-lagged TR variables to capture the dependence of flows in a given year on climatic conditions in previous years (Loaiciga et al., 1993). Where flashy discharge does not preclude the dendrohydrological approach, small watersheds may lend themselves to simpler TR-derived streamflow models based on a smaller number of predictors, as well as a lower probability of model over fitting. For this study, targeting the low-flow season enabled us to avoid the flashy winter high-flow period.

6.2. Reconstructed record and drought events

Generally, our reconstruction describes an historical pattern of intra-decadal high- and low-flow oscillations, with few sustained periods of very high or very low discharge. This lack of persistence is typical of a hybrid flow regime, and an important feature of the flow data for water management. It was critical that the zero-autocorrelation structure in our small study basins not be distorted by using TR data that contain biological persistence as model predictors, in this case through the use of residual chronologies (Meko and Woodhouse, 2011).

All of the seventeen reconstructed bottom fifth percentile flow years occurred prior to the hydrometric data period. With the exception of very low instrumental flows in 1985, sixteen of these events were more extreme than any in the gauged record (Fig. 6; Table 6). Our reconstruction suggests that pre-instrumental droughts were more severe than those in 1992, 1996, 2003, and 2009, when water scarcity throughout south coastal B.C. severely impacted municipal, hydroelectric, and agricultural water supplies (B.C. Ministry of Environment, 2010; Puska et al., 2011). The reconstructed record suggests both more severe worst-case scenario droughts, and a slightly higher probability of those droughts, than do the hydrometric data (Fig. 7). An important point in interpreting these results is that there is unexplained variance in the reconstruction, and a confidence interval around the low reconstructed flows, such that the true flows may have been lower. Further, reconstructed estimates of extremes are conservative due to expected variance compression, so that a reconstruction flow duration curve could typically show only less extreme values than a flow duration curve of observed streamflow values. It is therefore significant that the reconstruction curve suggests more likely, more severe droughts than the hydrometric curve. Especially given the accuracy of the model in estimating lowest flow magnitudes, our results suggest that: (1) extreme events cannot be reliably predicted based on the existing hydrometric flow record for hybrid watersheds in south coastal B.C.; and, (2) water management strategies based on these data are likely to underestimate worst-case scenario naturally occurring droughts.

Both mean winter and summer temperatures are projected to increase by 1.7 °C by 2050, while total summer precipitation is predicted to decrease by 13% (December–February; B.C. Ministry of Water, Land and Air Protection, 2002; Pike et al., 2010). It is not unreasonable to expect that future bottom fifth percentile-type natural low flows exacerbated by projected climate change-induced flow reductions could result in drought episodes of a severity unprecedented in the last ~350 years. We could not account for the extreme 2014 and 2015 droughts due to the unavailability of hydrometric data (B.C. Ministry of Forests, Lands and Natural Resource Operations, 2014).

Diagnostic correlation analyses supported the interpretation that lowest flows generally correspond with diminished snowpack and/or unusually warm and dry summer conditions. Depending on the fluctuating seasonal hydrology of hybrid regimes, hydrological drought may be caused by reduced winter snowpacks, increased summer temperature and aridity, or both. For example, inspection of the model predictor values in lowest flow years shows that the conspicuous droughts in 1682 and 1958 are coincident with large negative values of the PDSI, while 1674 and 1905 had very large TR index values expected during a year of reduced PAS.

6.3. Influences of ocean–atmosphere climate variability

The lack of relationship between the timing of high or low runoff with strong El Niño/La Niña events is surprising since, in the study region, warm dry El Niños typically reduce snowmelt-derived summer runoff while La Niñas enhance it (Fleming et al., 2007). ENSO fluctuations may not strongly determine regionally-synchronous runoff in the study streams, but it is more likely that either: (1) the sample size was too small for capturing real long-term relationships between ENSO and streamflow; or, (2) the influence of summer climate conditions, expressed by the PDSI, periodically 'overrides' that of winter conditions in determining summer runoff quantities. Visual inspection of time plots in Fig. 5 provides some indication of an overriding effect of summer conditions particularly during the warm PDO phase. The year-to-year association of gauged and estimated flows with PDSI during that phase is stronger than with PAS, including in years of enhanced snowpack followed by a warm/dry summer (e.g. 1985–1989). In contrast, the PAS and PDSI records generally "agree" during the cool phase; warm/dry conditions and cool/wet conditions persist from winter to summer (e.g. 1968–1971) so that streamflow is more strongly linked with PAS fluctuations during this phase. Although we could not assess these relationships quantitatively, they are consistent with the stronger—and in the case of the gauged record, significantly different—correlation of streamflow with winter PDO during the cool versus the warm phase, and with the role of PDO cool phases in enhancing snowmelt-derived runoff. The wavelet power spectrum exhibits some ENSO-type interannual variability intermittently throughout the reconstructed record, with loss of energy across all bandwidths during 1730–1760 and 1880–1910, while multi-decadal PDO-type variability is significant only during 1800–1850 (Fig. 7). Lower frequency variability may be absent as a result of detrending applied to the TR data.

6.4. Comparison with other paleorecords

The distinctly coastal nature of our study basins is reinforced by the general disagreement of our reconstruction with relevant paleoenvironmental records from continental western Canada and the United States, including a large number of streamflow reconstructions of continental, glacierized basins using precipitation-limited TRs (Axelson et al., 2009; Beriault and Sauchyn, 2006; Case and MacDonald, 2003; Gedalof et al., 2004; Sauchyn et al., 2014). Those records generally correspond with modes of ocean–atmosphere variability affecting continental environments and are consistent with historical north American-scale drought episodes (Cook et al., 2004; Stahle et al., 2007). Nor does our record resemble two streamflow reconstructions of non-hybrid basins in central-western B.C. (Hart et al., 2010; Starheim et al., 2013). A TR-derived reconstruction of May–July precipitation from the south coast of Vancouver Island presented by Jarett (2008) bears little resemblance to the streamflow record developed for this study,

likely due to the limited influence of precipitation during that season on July–August streamflow in the watersheds analyzed here.

6.5. Sources of unexplained variance

Choices relating to chronology development and regression model estimation, quality of the streamflow data, length of the calibration period, the inability of TRs to perfectly record climate fluctuations, and periodic decoupling of TR-climate relationships, may be responsible for a proportion of unexplained model variance. Uncertainty in the low-frequency component of streamflow variability is likely due to the detrending that we applied to the TR measurements. Sources of uncertainty not captured by the regression error variance include changes in watershed characteristics, undetected flow inputs lagged over years due to storage, and undetectable historical changes in the relationship between TR widths and climate. The model error of the reconstructed PDSI data is not explicitly accounted for in our regression modeling.

7. Conclusion

Our reconstruction indicates that recent droughts in hybrid watersheds in south coastal B.C. were not as severe as those that occurred naturally in the pre-instrumental period. Sixteen droughts occurred since 1658 that were more extreme than any in the gauged record. A frequency analysis of the reconstructed record suggests more severe worst-case scenario droughts and a slightly higher probability of those droughts than does a frequency analysis of the hydrometric data. This emphasizes both the usefulness of long-term records for probabilistic drought assessment, and the value of dendrohydrology as a source of long-term records. We suggest that water management strategies based on lowest observed flows determined from hydrometric data will underestimate the potential magnitudes of natural drought scenarios in these watersheds. In addition, if low-flow conditions anticipated under climate change exacerbate lowest possible natural flows, drought severities could exceed those in the past ~350 years. We reconstructed mean not minimum discharge values; actual low flow magnitudes would depart even further from mean flow values. We could not compare the extreme 2014 and 2015 droughts with preceding events due to a lack of hydrometric data.

Both gauged and reconstructed regionalized flows were negatively associated with fluctuations in winter PDO, most strongly during the PDO cool phase. The correlation of the gauged record with the PDO index was, in fact, significantly different during the cool versus warm phases, corroborating that summer discharge in hybrid streams is more strongly influenced by cool- than warm-phase PDO conditions as a result of increased snowmelt-derived runoff during cool phases (Fleming et al., 2007). We found no evidence of a statistical relationship between the timing of high or low runoff years with strong El Niño/La Niña events. This may have been due to an inability of the short comparable datasets to capture extant hydroclimate relationships. Alternatively, visual comparison of the streamflow data with PAS and PDSI records suggested an overriding influence of summer climate conditions over snowmelt quantities during the PDO warm phase, which could account for weak runoff–PDO linkages during that phase. Our reconstruction is distinctly coastal in flavor. It is incongruous with paleohydrological records from continental environments or records of spring precipitation and snowmelt-dominated streamflow as a result of the inconsistent year-to-year influence of snowmelt on hybrid stream discharge.

From a model-development standpoint, we demonstrate that TR-based reconstruction of small hybrid basins in temperate environments can be optimized using a combination of PAS and summer drought sensitive proxies as model predictors. Our model hindcasts synchronous variability in summer discharge among the four study streams over the interval 1658–1990, and explains 64% of the discharge variance over the 1960–1990 model calibration period. Targeting the low-flow season enabled us to avoid high and flashy winter flows that cannot not be modeled using TRs in the study environment, while the lack of year-to-year persistence in the flow data made these watersheds amenable to a simple paleohydrological model based on a smaller number of predictors and minimized the probability of model over fitting. This study represents the first attempt to develop a paleohydrological model of regionally-synchronous streamflow in B.C., and to our knowledge provides the strongest annually resolved paleoenvironmental record of streamflow in the province.

Acknowledgements

Funding for this research was provided by Natural Sciences and Engineering Research Council of Canada (NSERC) awards to Coulthard (Alexander Graham Bell Canada Graduate Scholarship CGS-D, Michael Smith Foreign Study Supplement) and a Discovery Grant awarded to Smith. The authors wish to thank the Laboratory of Tree-Ring Research at the University of Arizona for hosting Coulthard in Spring 2013, and Malcolm Hughes, Justin DeRose, Matt Bekker, and Dan Griffin for helpful comments in the development of this paper. We also wish to acknowledge the data collection efforts of Colin Laroque.

References

Agriculture and Agri-Food Canada, 2014. 2014 Annual Review of Agroclimate Conditions Across Canada. From <http://www.agr.gc.ca/eng/?id=1399580648022> (retrieved May 1, 2015).

Axelson, J., Sauchyn, D.J., Barichivich, J., 2009. New reconstructions of streamflow variability in the South Saskatchewan River basin from a network of tree ring chronologies, Alberta, Canada. Water Resour. Res. 45 (W09422). http://dx.doi.org/10.1029/2008WR007639.

Barnett, T., Malone, R., Pennell, W., Stammer, D., Semter, B., Washington, W., 2004. The effects of climate change on water resources in the West: introduction and overview. Clim. Change 62 (1), 1–11.

B.C. Conservation Foundation, 2006. Vancouver Island Focus Watersheds: Trent and Tsable rivers. From <http://www.bccf.com/steelhead/focus5.htm> (retrieved September 25, 2013).

B.C. Ministry of Environment, 2010. Preparing for Climate Change: British Columbia's Adaptation Strategy. From <http://www2.gov.bc.ca/gov/DownloadAsset?assetId=29CDF35B126E483A966B0D5DAE2E3E38&filename=adaptation_strategy.pd> (retrieved September 25, 2013).

B.C. Ministry of Environment, Water Protection and Sustainability Branch, 2013. A Water Sustainability Act for B.C.: legislative proposal overview. From <http://engage.gov.bc.ca/watersustainabilityact/files/2013/10/WSA_overview_web.pdf> (retrieved October 14, 2014).

B.C. Ministry of Forests, Lands and Natural Resource Operations, 2014. Water Supply and Streamflow Conditions Bulletin. From <http://bcrfc.env.gov.bc.ca/bulletins/watersupply/index-watersupply.htm> (retrieved July 19, 2014).

B.C. Ministry of Water, Land and Air Protection, 2002. Indicators of climate change for British Columbia, 2002. From <http://www.env.gov.bc.ca/cas/pdfs/indcc.pdf> (retrieved September 25, 2013).

B.C. River Forecast Centre, 2015. Snow Survey and Water Supply Bulletin. From <http://bcrfc.env.gov.bc.ca/bulletins/watersupply/current.htm> (retrieved June 20, 2015).

Beaulieu, M., Schreier, H., Jost, G., 2012. A shifting hydrological regime: a field investigation of snowmelt runoff processes and their connection to summer base flow, Sunshine Coast, British Columbia. Hydrol. Process. 26 (17), 2672–2682.

Beriault, A.L., Sauchyn, D.J., 2006. Tree-ring reconstructions of streamflow in the Churchill River Basin, northern Saskatchewan. Can. Water Resour. J. 31 (4), 249–262.

Biondi, F., Strachan, S., 2012. Dendrohydrology in 2050: challenges and opportunities. In: Grayman, W., Loucks, D., Saito, L. (Eds.), Toward a Sustainable Water Future: Visions for 2050. American Society of Civil Engineers, Reston, VA, pp. 355–362.

Bonfils, C., Santer, B., Pierce, D., Hidalgo, H., Bala, G., Das, T., Barnett, T., Cayan, D., Doutriaux, C., Wood, A., Mirin, A., Nozawa, T., 2008. Detection and attribution of temperature changes in the mountainous western United States. J. Clim. 21 (23), 6404–6424.

Bonsal, B., Shabbar, A., 2008. Impacts of large-scale circulation variability on low streamflows over Canada: a review. Can. Water Resour. J. 33 (2), 137–154.

Box, G., Jenkins, G., 1976. Time Series Analysis: Forecasting and Control, revised ed. Holden-Day, Oakland CA.
Bunn, A.G., 2008. A dendrochronology program library in R (dplR). Dendrochronologia 26 (2), 115–124.
Case, R.A., MacDonald, G.M., 2003. Tree ring reconstructions of streamflow for three Canadian prairie rivers. JAWRA J. Am. Water Resour. Assoc. 39 (3), 703–716.
Cook, E.R., Holmes, R.L., 1986. Users Manual for Program ARSTAN. Laboratory of Tree-Ring Research, University of Arizona, Tucson, USA.
Cook, E.R., Woodhouse, C., Eakin, C.M., Meko, D.M., Stahle, D.W., 2004. Long-term aridity changes in the western United States. Science 306 (5698), 1015–1018.
Cook, E., Kairiūkštis, L. (Eds.), 1990. Methods of Dendrochronology: Applications in the Environmental Sciences. Kluwer Academic Publishers, Netherlands.
Cook, E.R., Peters, K., 1981. The smoothing spline: a new approach to standardizing forest interior tree-ring width series for dendroclimatic studies. Tree-Ring Bull. 41 (1), 45–53.
Cook, E.R., Meko, D.M., Stahle, D.W., Cleaveland, M.K., 1999. Drought reconstructions for the continental United States. J. Clim. 12 (4), 1145–1162.
Coulthard, B., Smith, D.J., 2015. A 477-year dendrohydrological assessment of drought severity for Tsable River, Vancouver Island, British Columbia, Canada. Hydrol. Process. http://dx.doi.org/10.1002/hyp.10726.
Craig, J.D.C., 2004. Construction of artificial fish habitat in the Chemainus River, 2004. Report Prepared for BC Conservation Foundation: Greater Georgia Basin Steelhead Recovery Plan, Nanaimo, BC. From <http://www.bccf.com/steelhead/pdf/Chemainus_R_artificial_fish_habitat_2004%20new.pdf> (retrieved September 25, 2013).
D'Agostino, R.B., Pearson, E.S., 1973. Tests for departure from Normality. Biometrika 60, 613–622.
Daly, C., Gibson, W., Taylor, G., 2002. A knowledge-based approach to the statistical mapping of climate. Clim. Res. 22 (2), 99–113.
Dawdy, D., Matalas, N., 1964. Statistical and probability analysis of hydrologic data, part III: Analysis of variance, covariance and time series. In: Chow, V.T. (Ed.), Handbook of Applied Hydrology, A Compendium of Water-Resources Technology. McGraw-Hill, New York, NY, pp. 8.68–8.90.
Déry, S.J., Stahl, K., Moore, R.D., Whitfield, P.H., Menounos, B., Burford, J.E., 2009. Detection of runoff timing changes in pluvial, nival, and glacial rivers of western Canada. Water Resour. Res. 45 (W06701). http://dx.doi.org/10.1029/2009WR008244.
Earle, C., 1993. Asynchronous droughts in California streamflow as reconstructed from tree rings. Quatern. Res. 39 (3), 290–299.
Eaton, B., Moore, R., 2010. Regional hydrology. In: Pike, R.G., Redding, T.E., Moore, R.D., Winkler, R.D., Bladon, K.D. (Eds.), Compendium of Forest Hydrology and Geomorphology in British Columbia. Ministry of Forests and Range Research Branch/FORREX Forest Research Extension Partnership, Victoria, BC, pp. 85–110.
Fleming, S.W., Whitfield, P.H., Moore, R.D., Quilty, E.J., 2007. Regime-dependent streamflow sensitivities to Pacific climate modes cross the Georgia-Puget transboundary ecoregion. Hydrol. Process. 21 (24), 3264–3287.
Fritts, H.C., 1976. Trees and Climate. Academic Press Inc., London.
Fritts, H., 1990. Modeling tree-ring and environmental relationships for dendrochronological analysis. In: Dixon, R., Meldahl, R., Ruark, G., Warren, W. (Eds.), Process Modeling of Forest Growth Responses to Environmental Stress. Timber Press, Portland, OR, pp. 368–382.
Gaboury, M., McCulloch, M., 2002. Fish habitat restoration designs for five east Vancouver Island watersheds. Report prepared for BC Conservation Foundation, Nanaimo BC. From <http://a100.gov.bc.ca/appsdata/acat/documents/r5855/FishHabitatRestorationDesignsfor5ECVIWatersheds_1143409089471_d65067ddb3744fadbb2db077cc5c960e.pdf> (retrieved September 25, 2013).
Gedalof, Z., Peterson, D., Mantua, N., 2004. Columbia river flow and drought since 1750. JAWRA J. Am. Water Resour. Assoc. 40 (6), 1579–1592.
Gedalof, Z., Smith, D.J., 2001. Dendroclimatic response of mountain hemlock (*Tsuga mertensiana*) in Pacific North America. Can. J. For. Res. 31 (2), 322–332.
Gou, X., Deng, Y., Chen, F., Yang, M., Fang, K., Gao, L., Yang, T., Zhang, F., 2010. Tree ring based streamflow reconstruction for the Upper Yellow River over the past 1234 years. Chin. Sci. Bull. 55 (36), 4179–4186.
Grissino-Mayer, H.D., 2001. Research report evaluating crossdating accuracy: a manual and tutorial for the computer program COFECHA. Tree-Ring Res. 57 (1), 115–124.
Hamlet, A.F., Lettenmaier, D.P., 1999. Columbia river streamflow forecasting based on ENSO and PDO climate signals. J. Water Resour. Plann. Manage. 125 (6), 333–341.
Hart, S.J., Smith, D.J., Clague, J.J., 2010. A multi-species dendroclimatic reconstruction of Chilko River streamflow, British Columbia, Canada. Hydrol. Process. 24 (19), 2752–2761.
Holmes, R.L., 1983. Computer-assisted quality control in tree-ring dating and measurement. Tree-Ring Bull. 43 (1), 69–78.
Holton, J.R., Dmowska, R., 1989. In: Philander, S.G. (Ed.), El Niño, La Niña, and the southern oscillation, vol. 46. Academic Press.
Jarett, T., 2008. A dendroclimatic investigation of moisture variability and drought in the Greater Victoria Water Supply Area, Vancouver Island, British Columbia. Master's Thesis. University of Victoria, Victoria, British Columbia, Canada. From <https://dspace.library.uvic.ca//handle/1828/883> (retrieved March 4, 2015).
Kachigan, S., 1982. Multivariate Statistical Analysis: A Conceptual Introduction. Radius Press, New York, NY.
Kanaka Creek Regional Park Management Plan, 2004. Report prepared by the Greater Vancouver Regional District, Vancouver, BC. From <http://www.metrovancouver.org/services/parks/ParksPublications/KanakaManagementPlan.pdf> (retrieved September 25, 2013).
Kay, J., Blecic, B., 1996. Chemainus River Water Allocation Plan. Province of British Columbia Ministry of Environment, Lands, and Parks, Nanaimo, BC.
Kiffney, P., Bull, J., Feller, M., 2002. Climatic and hydrologic variability in a coastal watershed of southwestern British Columbia. JAWRA J. Am. Water Resour. Assoc. 38 (5), 1437–1451.
Klinka, K., Pojar, J., Meidinger, D., 1991. Revision of biogeoclimatic units of coastal British Columbia. Northwest Sci. 65 (1), 32–47.
Laroque, C.P., Smith, D.J., 1999. Tree-ring analysis of yellow cedar (*Chamaecyparis nootkatensis*) on Vancouver Island British Columbia. Can. J. For. Res. 29 (1), 115–123.
Laroque, C., Smith, D., 2003. Radial-growth forecasts for five high-elevation conifer species on Vancouver Island, British Columbia. For. Ecol. Manage. 183 (1), 313–325.
Lill, A., 2002. Greater Georgia Basin steelhead recovery action plan. Report prepared for BC Conservation Foundation: Greater Georgia Basin Steelhead Recovery Plan, Nanaimo, BC. From <http://www.bccf.com/steelhead/pdf/Steelheadreport092702.pdf> (retrieved September 25, 2013).
Loaiciga, H., Haston, A., Michaelsen, J., 1993. Dendrohydrology and long-term hydrologic phenomena. Rev. Geophys. 31 (2), 151–171.
Loukas, A., Vasiliades, L., Dalezios, N., 2002. Climatic impacts on the runoff generation processes in British Columbia, Canada. Hydrol. Earth Syst. Sci. Discuss. 6 (2), 211–228.
Mantua, N., 2002. Pacific-decadal oscillation. In: MacCracken, M., Perry, J.S. (Eds.), Encyclopedia of Global Environmental Change, vol. 1. John Wiley and Sons, Chichester, UK, pp. 592–594.
Mantua, N., Tohver, I., Hamlet, A., 2010. Climate change impacts on streamflow extremes and summertime stream temperature and their possible consequences for freshwater salmon habitat in Washington State. Clim. Change 102 (1–2), 187–223.
Marcinkowski, K., Peterson, D.L., Ettl, G.J., 2015. Nonstationary temporal response of mountain hemlock growth to climatic variability in the North Cascade Range, Washington, USA. Can. J. For. Res. 45 (999), 676–688.
Margolis, E., Meko, D., Touchan, R., 2011. A tree-ring reconstruction of streamflow in the Santa Fe River, New Mexico. J. Hydrol. 397 (1), 118–127.
Mays, L.M., 2005. Water Resources Engineering. Wiley & Sons, New York, NY.
Means, J.E., 1990. Tsuga mertensiana (Bong.) Carr. mountain hemlock. In: Silvics of North America, vol. 1, pp. 623–631.
Meko, D., Therrell, M., Baisan, C., Hughes, M.K., 2001. Sacramento River flow reconstructed to AD. 869 from tree rings. J. Am. Water Resour. Assoc. 37 (4), 1029–1039.
Meko, D., Graybill, D., 1995. Tree-ring reconstruction of upper Gila River discharge. JAWRA J. Am. Water Resour. Assoc. 31 (4), 605–616.
Meko, D., Touchan, R., Anchukaitis, K., 2011. Seascorr: a MATLAB program for identifying the seasonal climate signal in an annual tree-ring time series. Comput. Geosci. 37 (9), 1234–1241.
Meko, D., Woodhouse, C., 2011. Application of streamflow reconstruction to water resources management. In: Hughes, M.K., Swetnam, T.W., Diaz, H.F. (Eds.), Dendroclimatology. Springer, Netherlands, pp. 231–261.
Michaelsen, J., 1987. Cross-validation in statistical climate forecast models. J. Clim. Appl. Meteorol. 26 (11), 1589–1600.
Mishra, A., Coulibaly, P., 2009. Developments in hydrometric network design: a review. Rev. Geophys. 47 (RG2001). http://dx.doi.org/10.1029/2007RG000243.
Moore, R.D., Allen, D.M., Stahl, K., 2007. Climate change and low flows: influences of groundwater and glaciers. Final Report Prepared for Climate Change Action Fund, Natural Resources Canada, Vancouver, BC. From <https://www.sfu.ca/personal/dallen/CCAF_A875-FinalReport.pdf> (retrieved September 25, 2013).
Mosteller, F., Tukey, J., 1977. Data Analysis and Regression: A Second Course in Statistics. Addison-Wesley Publishing Company, Reading, MA.
Mote, P.W., Parson, E.A., Hamlet, A.F., Keeton, W.S., Lettenmaier, D., Mantua, N., Miles, E.L., Peterson, D.W., Peterson, D.L., Slaughter, R., Snover, A.K., 2003. Preparing for climatic change: the water, salmon, and forests of the Pacific northwest. Clim. Change 61 (1–2), 45–88.
Nelitz, M., Alexander, C.A., Wieckowski, K., Council, P.F.R.C., 2007. Helping Pacific salmon survive the impact of climate change on freshwater habitats: case Studies. Final Report Prepared for Pacific Fisheries Resource Conservation Council, Vancouver, BC. Retrieved from <https://www.sfu.ca/personal/dallen/CCAF_A875-FinalReport.pdf>.
Newcombe, R.G., 1998. Interval estimation for the difference between independent proportions: comparison of eleven methods. Stat. Med. 17 (8), 873–890.
North, G.R., Bell, T.L., Cahalan, R.F., Moeng, F.J., 1982. Sampling errors in the estimation of empirical orthogonal functions. Monthly Weather Rev. 110 (7), 699–706.
Norton, D.A., Palmer, J.G., 1992. Dendroclimatic evidence from Australasia. In: Bradley, R.S., Jones, P.D. (Eds.), Climate Since AD 1500. Routledge, New York, NY, pp. 463–481.
Palmer, W., 1965. Meteorological Drought. US Department of Commerce, Weather Bureau, Washington, DC.
Pederson, N., Jacoby, G.C., D'Arrigo, R.D., Cook, E.R., Buckley, B.M., Dugarjav, C., Mijiddorj, R., 2001. Hydrometeorological reconstructions for Northeastern Mongolia derived from tree rings: 1651–1995. J. Clim. 14 (5), 872–881.
Peterson, D.W., Peterson, D.L., 1994. Effects of climate on radial growth of subalpine conifers in the North Cascade Mountains. Can. J. For. Res. 24 (9), 1921–1932.
Peterson, D.W., Peterson, D.L., 2001. Mountain hemlock growth responds to climatic variability at annual and decadal time scales. Ecology 82 (12), 3330–3345.
Pike, R., Bennett, K., Redding, T., Werner, A.T., Spittlehouse, D.L., Moore, R.D., Murdock, T.Q., Beckers, J., Smerdon, B.D., Bladon, K.D., Foord, V.N., Campbell, D.

A., Tschaplinski, P.J., 2006. Climate change effects on watershed processes in British Columbia. In: Pike, R.G., Redding, T.E., Moore, R.D., Winkler, R.D., Bladon, K.D. (Eds.), Compendium of Forest Hydrology and Geomorphology in British Columbia. Ministry of Forests and Range Research Branch/FORREX Forest Research Extension Partnership, Victoria, BC, pp. 699–747.

Pike, R., Spittlehouse, D., 2008. Climate change and watershed hydrology: Part I–recent and projected changes in British Columbia. Streamline Watershed Manage. Bull. 11 (2), 1–8.

Pojar, J., Klinka, K., Demarchi, D.A., 1991. Mountain hemlock zone. In: Meidinger, D., Pojar, J. (Eds.), Ecosystems of British Columbia. Ministry of Forests, Victoria, BC, pp. 113–124.

Poulin, V., 2005. Vancouver Island riparian restoration recommendation and prescriptions–Quinsam, Chemainus, Englishman, Little Qualicum, and Oyster Rivers. Report Prepared for BC Conservation Foundation: Greater Georgia Basin Steelhead Recovery Plan, Nanaimo, BC. From <http://www.bccf.com/steelhead/pdf/vi_riparian_prescription_report_final_2005.pdf> (retrieved September 25, 2013).

Puska, L., Clements, L., Chandler, K., 2011. Climate change and food security on Vancouver Island: discussion paper. Report Prepared by Vancouver Island Local Food Project, Victoria, BC. From <http://www.uvic.ca/research/centres/cue/assets/docs/Climate%20Change%20and%20Food%20Report.pdf> (retrieved March 4, 2015).

Rodenhuis D.R., Bennett, K.E., Werner, A.T., Murdock, T.Q., Bronaugh, D., 2007. Climate overview 2007: hydro-climatology and future climate impacts in British Columbia. Report Prepared by the Pacific Climate Impacts Consortium, Victoria, BC. From <http://www.pacificclimate.org/sites/default/files/publications/Rodenhuis.ClimateOverview.Mar2009.pdf> (retrieved September 25, 2013).

Sauchyn, D.J., Vanstone, J., St. Jacques, J.-M., Sauchyn, R., 2014. Dendrohydrology in Canada's western interior and applications to water resource management. J. Hydrol. http://dx.doi.org/10.1016/j.jhydrol.2014.11.049.

Schnorbus, M., Werner, A., Bennett, K., 2014. Impacts of climate change in three hydrologic regimes in British Columbia, Canada. Hydrol. Process. 28 (3), 1170–1189.

Smith, D.J., Laroque, C.P., 1998. High-elevation dendroclimatic records from Vancouver Island. In: MacIver, D., Meyer, R.E. (Eds.), Proceedings of the Workshop on Decoding Canada's Environmental Past: Climate Variations and Biodiversity Change during the Last Millennium. Atmospheric Service, Environment Canada, Downsview, Ont, pp. 33–44.

Snedecor, G.W., Cochran, W.G., 1989. Statistical Methods, eighth ed. Iowa State University, Ames, IA.

Snee, R.D., 1977. Validation of regression models: methods and examples. Technometrics 19 (4), 415–428.

Stahl, K., Moore, R.D., Mckendry, I.G., 2006. The role of synoptic-scale circulation in the linkage between large-scale ocean–atmosphere indices and winter surface climate in British Columbia, Canada. Int. J. Climatol. 26 (4), 541–560.

Stahle, D., Fye, F., Cook, E., Griffin, R.D., 2007. Tree-ring reconstructed megadroughts over North America since AD 1300. Clim. Change 83 (1–2), 133–149.

Starheim, C.C.A., Smith, D.J., Prowse, T.D., 2013. Dendrohydroclimate reconstructions of July–August runoff for two nival-regime rivers in west central British Columbia. Hydrol. Process. 27 (3), 405–420.

Stewart, I., Cayan, D., Dettinger, M., 2005. Changes toward earlier streamflow timing across western North America. J. Clim. 18 (8), 1136–1155.

Wigley, T.M.L., Briffa, K.R., Jones, P.D., 1984. On the average value of correlated time series, with applications in dendroclimatology and hydrometeorology. J. Appl. Meteorol. 23 (2), 201–213.

Torrence, C., Compo, G., 1998. A practical guide to wavelet analysis. Bull. Am. Meteorol. Soc. 79 (1), 61–78.

Valentine, K.W.G., Sprout, P.N., Baker, T.E., Lawkulich, L.M. (Eds.), 1978. The Soil Landscapes of British Columbia. BC Ministry of Environment, Resource Analysis Branch, 197 p.

Van Lanen, H.A.J., Wanders, N., Tallaksen, L.M., Van Loon, A.F., 2013. Hydrological drought across the world: impact of climate and physical catchment structure. Hydrol. Earth Syst. Sci. 17, 1715–1732.

Van Loon, A.F., Laaha, G., 2015. Hydrological drought severity explained by climate and catchment characteristics. J. Hydrol. 256 (1), 3–14.

Venables, W., Ripley, B., 2002. Modern Applied Statistics Using S. Springer-Verlag.

Wade, N., Martin, J., Whitfield, P., 2001. Hydrologic and climatic zonation of Georgia basin, British Columbia. Can. Water Resour. J. 26 (1), 43–70.

Wang, T., Hamann, A., Spittlehouse, D.L., Murdock, T.Q., 2012. ClimateWNA-high-resolution spatial climate data for western North America. J. Appl. Meteorol. Climatol. 51 (1), 16–29.

Watson, E., Luckman, B.H., 2005. Spatial patterns of preinstrumental moisture variability. J. Clim. 18 (15), 2847–2863.

Whitfield, P., Cannon, A., 2000. Recent variations in climate and hydrology in Canada. Can. Water Resour. J. 25 (1), 19–65.

Weisberg, S., 1985. Applied Linear Regression, second ed. John Wiley, New York, NY.

Woodhouse, C.A., Lukas, J.J., 2006. Drought, tree rings and water resource management in Colorado. Can. Water Resour. J. 31 (4), 297–310.

Young, J., Werring, J., 2006. The will to protect: preserving BC's Wild Salmon habitat. Report Prepared for the David Suzuki Foundation. From <http://www.davidsuzuki.org/publications/downloads/2006/DSF-Will_to_Protect-72.pdf> (retrieved September 25, 2013).